Effect of Facesheet Thickness on Dynamic Response of Composite Sandwich Plates to Underwater Impulsive Loading

S. Avachat and M. Zhou

The George W. Woodruff School of Mechanical Engineering
School of Materials Science and Engineering
Georgia Institute of Technology
Atlanta, GA 30332-0405, USA
e-mail: min.zhou@gatech.edu

Keywords: Sandwich structures, composites, dynamic response, underwater impulsive loading

Introduction

Ships, submersibles and other marine structures are susceptible to damage due to dynamic loading from underwater explosions, projectile impact and hull slamming resulting from high-speed motion. By virtue of the combination of a thick core and thin facesheets, sandwich structures achieve considerably high shear-stiffness-to-weight ratios and bending-stiffness-to-weight ratios than equivalent homogeneous plates made exclusively of the core material or the facesheet material. The primary factors that influence the structural response of a sandwich structure are (1) facesheet thickness, (2) core thickness and (3) core density. The bulk of previous research on the dynamic behavior of sandwich composites has focused on low-velocity contact-based loads such as drop weight and projectile impact [1-7]. Experimental studies aimed at understanding material and structural responses under blast loads have been carried out [8-10]. Espinosa et al. simulated underwater blasts by impacting a projectile on a piston in contact with water [11, 12] and concluded that steels may be preferred when maintenance of residual strength is a priority and composite materials make better low-weight blast-resistant hulls. The objective of this study is to examine the effect of the ratio between facesheet thickness and core thickness on the dynamic response of composite sandwich structures. To this end, the core thickness and core density are kept constant and the thickness of the facesheets is varied so that the total mass of the structure changes in every configuration. Under this condition, the total mass of the structure changes with the increase in facesheet thickness.

Experimental Configuration

Gas gun impact has been successfully used to generate impulsive loading through water [11, 13, 14]. Important features of our facility include the ability to generate water-based impulsive loading of a wide-range of intensities, the ability to simulate the loading of submerged structures, and integrated high-speed photographic and laser interferometric diagnostics. This facility is used in conjunction with computational modeling. Figures 1 (a) shows a schematic illustration of the experimental configuration analyzed in this paper. A projectile is accelerated by the gas gun and impacts the piston plate, generating a planar pressure pulse in the shock tube. Depending on the projectile velocity, pressures ranging from 10 to 300 MPa can be generated in the shock tube. The cylindrical shape of the shock tube allows an essentially uniform pressure to be applied to the target over the area of contact. Figure 1 (b) shows the pressure histories corresponding to five different projectile velocities, as predicted by the simulations. Impulse I is calculated as $I = \int p \cdot dt$, where p is the pressure, t is the decay time. The five impulse magnitudes considered in the simulations are 42, 30, 18, 12 and 4 kPa·s.

Materials

The core is made of Divinycell H-100 PVC foam [15] whose response is described by a volumetric hardening model in which the evolution of the yield surface is driven by the volumetric plastic strain [16]. The constitutive model adopted for Dinvinycell H100 PVC foam is the one developed by Zhang et al. [17] and implemented in the current finite element code [18, 19]. The facesheets are made of a glass fiber reinforced epoxy composite. Each facesheet consists of plies in a bi-axial $[0/90]_S$ layup and is modeled with the Hashin damage model with energy-based damage evolution [20]. All panels have a core thickness of T_c = 20 mm and a core density of ρ_c = 100 kg/m^3, giving a core unit areal mass of M_c = 2 kg/m^2. The side length of the plate is L = 300 mm. The facesheets, consisting of plies 0.25 mm in thickness each, are modeled with continuum shell

elements. The total facesheet thickness T_f varies from 1 to 20 mm, giving rise to different areal mass values of the sandwich plates. The ratio between the facesheet thickness and the core thickness is $R = T_f / T_c$ and the value of T_f / T_c ranges from 0.05 to 1.

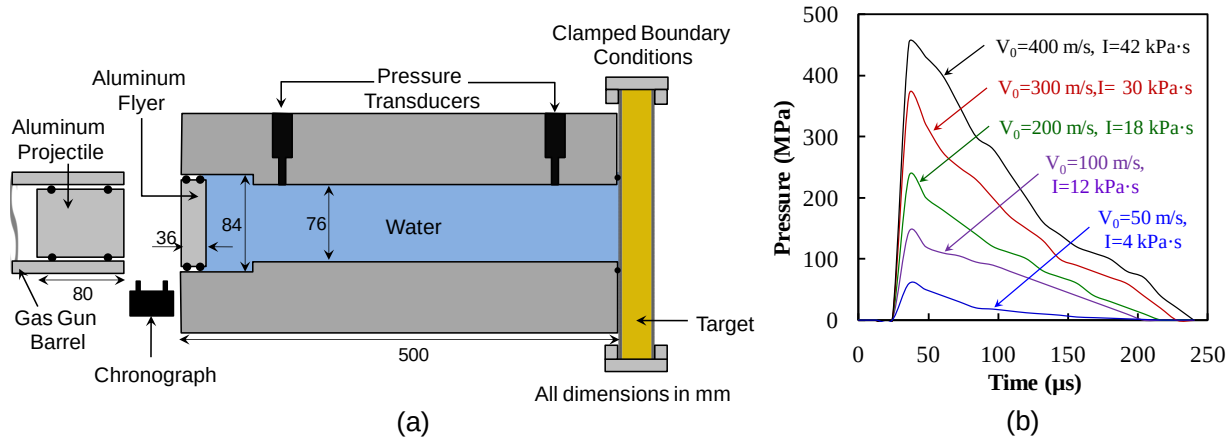

Figure 1 (a) schematic of loading configuration for a clamped sandwich plate; (b) pressure profiles for the five projectile velocities.

Finite Element Model

The numerical model explicitly accounts for the projectile, piston plate and water column in contact with the sandwich plate target. A $[0/90]_S$ layup is specified for each ply in the facesheets. A master-slave contact algorithm is used for interactions between the facesheets and core and a non-penetrating, general contact algorithm is implemented at projectile-piston, piston-water and water-sandwich structure interfaces. Cohesive elements are used at the core-facesheet interfaces to simulate core-facesheet debonding [18, 21]. A bilinear cohesive law is implemented, accounting for mixed-mode failure at the interfaces. A normal penalty-based contact algorithm is used to prevent interpenetration of crack surfaces. The following quantities are tracked to quantify and compare the responses of the sandwich plates:

I. the displacements at the center of facesheets 1 and 2;
II. core crushing rate and core crushing strain;
III. energy dissipated in the structure; and
IV. compressive and tensile damages in the facesheets.

Results

A large number of calculations have been carried out. The deformation of the core shows three distinct stages of response: (1) onset of core crushing, (2) onset of motion of back face and (3) momentum transfer through the structure. Changes made to the facesheets affect all three stages. In general, all things being equal, structures with thicker facesheets are stronger in an absolute sense, since more material is used. To reveal trends on a per weight basis, we analyze the results in both normalized and non-normalized forms. For the five impulse levels per unit area considered ($I = 4\,\text{kPa}\cdot\text{s}$, $I = 12\,\text{kPa}\cdot\text{s}$, $I = 18\,\text{kPa}\cdot\text{s}$, $I = 30\,\text{kPa}\cdot\text{s}$ and $I = 42\,\text{kPa}\cdot\text{s}$), we first focus on the results for $I = 18\,\text{kPa}\cdot\text{s}$ and then compare the results for the different impulse levels.

The Hashin damage model for fiber-reinforced composites takes into account tensile and compressive damage. Figures 2 (a) - (d) show the distribution of damage parameter F^t_m in the last ply in the composite layup in facesheets-1 and 2. Note that what is shown is not the cumulative damage in an entire facesheet. Rather, the figures show damages in the ply in each of the facesheets that is farthest away from the front face of the sandwich specimen. The distribution and severity of damage facilitate comparison of the results for different T_f/T_c ratios under identical loading conditions. Figure 2 (a) shows the distribution of tensile damage in the matrix for the last ply of the facesheet-1, 600 μs after onset

of deformation in a sandwich plate with a facesheet thickness of 8 mm ($T_f/T_c = 0.4$). The load intensity is $I = 18\,\text{kPa}\cdot\text{s}$. Damage in the front sheet (facesheet 1) is more severe and is dependent on fiber orientation. Maximum damage occurs close to the loading area and spreads outward in later stages of the loading event. Figure 2(c) shows the tensile damage in the matrix for the final ply of the facesheets in a sandwich structure with a facesheet thickness of 1 mm ($T_f/T_c = 0.05$). While the damages in facesheet 1 for both $T_f/T_c = 0.05$ (Fig. 2 (a)) and $T_f/T_c = 0.4$ (Fig. 2 (c)) are similar, the damages in facesheet 2 are quite different, with the damage for $T_f/T_c = 0.4$ (Fig. 2 (b)) being much lower than that for $T_f/T_c = 0.05$ (Fig. 2 (d)). Beyond $T_f/T_c = 0.4$, there is essentially no further improvement in damage resistance. Like damage in the facesheets, core-facesheet debonding is more severe for thin facesheets.

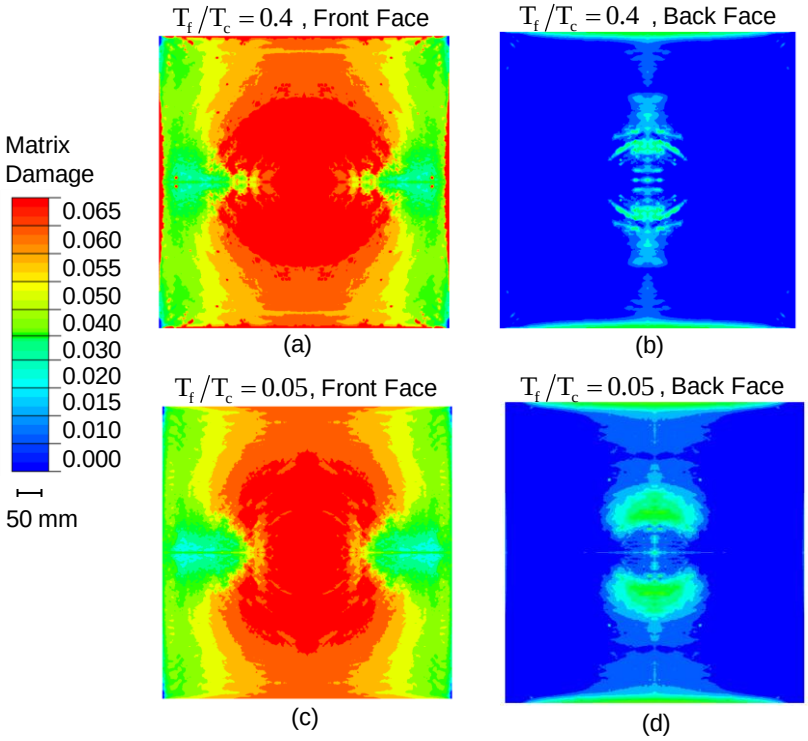

Figure 2 Distributions of tensile matrix damage for T_f/T_c = 4 and T_f/T_c = 0.05 for I = 18 kPa·s.

Deflection

The duration of loading on the target is approximately 250 μs. The displacements at the center of the structures are used to quantify deflection and core compression. In particular, the displacements at the center of the front and back facesheets (Δ) at 600 μs after the onset of loading are analyzed. The deflections are normalized with the side length (L) of the sandwich plates. Figure 3 shows that Δ/L increases with I and decreases with the ratio between the thickness of the facesheets and the thickness of the core (T_f/T_c) [and therefore decreases with the areal mass of sandwich plates (M)]. The deflection of facesheet 2 is generally lower than that of facesheet 1, due to core compression. As T_f/T_c increases, the decreases in deflections are monotonic. At low impulse magnitudes ($I < 12\,\text{kPa}\cdot\text{s}$), increasing facesheet thickness does not provide significant reductions in the deflections. As the impulse magnitude increases, the difference between the responses of structures with low T_f/T_c and the responses of those with high T_f/T_c becomes pronounced. For impulse magnitudes above $12\,\text{kPa}\cdot\text{s}$, structures with high T_f/T_c values show markedly lower deflections. For

example at $I = 18, 30, 42\ \text{kPa}\cdot\text{s}$, as $\text{T}_\text{f}/\text{T}_\text{c}$ increases from 0.01 to 0.36, Δ/L decreases by approximately 56 %. If $\text{T}_\text{f}/\text{T}_\text{c}$ increases from 0.6 to 1, Δ/L decreases by only ~5 %. At all impulse magnitudes, no appreciable reduction in the deflection of facesheet 1 is seen for $\text{T}_\text{f}/\text{T}_\text{c} > 0.6$. The deflections of facesheet 2 shown in Fig. 3 (b) are generally lower that the deflections of facesheet 1 but exhibit the same trend seen in Fig. 3 (a). Overall, increasing the relative thickness of the facesheets up to a certain value ($\text{T}_\text{f}/\text{T}_\text{c} = 0.6$) can significantly decrease the deformation of the structures. Increases beyond this value yields no obvious benefit in terms of structural rigidity. Since the overall weight of the structures is one of the most important aspects in naval structural design, this finding points to a design criterion useful for relevant systems.

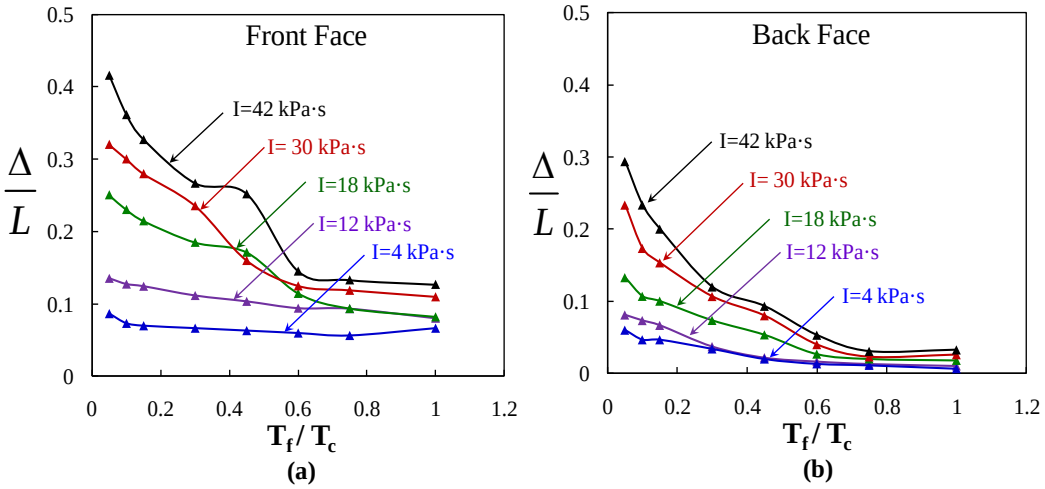

Figure 3 Normalized displacement as a function of T_f/T_c for (a) front facesheet (facesheet 1) and (b) back facesheet (facesheet 2).

Energy Absorption

Energy dissipation in glass-fiber reinforced composites is in the form of matrix cracking, fiber breakage and delamination. In the current analysis, only matrix and fiber damages are considered. Energy absorption in the core is in the form of permanent core compression which accounts for the largest portion of overall energy dissipated. For the load conditions analyzed, the primary mode of core deformation is compression with very small amounts of stretching at the supports. Therefore, taking full advantage of core compression is important. Calculations of the dissipated work associated with different deformation and damage mechanisms are described in [18]. Figure 4 (a) shows the total energy dissipated in the structure (U) as a function of T_f/T_c. For thin facesheets ($\text{T}_\text{f}/\text{T}_\text{c} < 0.15$), the core compression is highly localized to the load area, leaving large portions of the core relatively intact or underused. For $0.15 < \text{T}_\text{f}/\text{T}_\text{c} < 0.45$, the facesheets are rigid enough to distribute core compression over a larger area, whereby achieving maximum energy dissipation. For $\text{T}_\text{f}/\text{T}_\text{c} > 0.6$, no further improvement in energy dissipation can be gained at all impulse magnitudes, since the core is already fully utilized. An interesting aspect of this plot is that *U* reaches a maximum at a certain value of T_f/T_c, indicating that there is an optimum thickness ratio (approximately $\text{T}_\text{f}/\text{T}_\text{c} = 0.2 - 0.3$) for maximizing energy dissipation. This maximum becomes more obvious at higher load intensities. Figure 4 (b) shows the energy dissipated per unit areal mass (U/M) as a function of $\text{T}_\text{f}/\text{T}_\text{c}$ for different load intensities. As the $\text{T}_\text{f}/\text{T}_\text{c}$ increases, U/M decreases significantly and eventually levels off at around $\text{T}_\text{f}/\text{T}_\text{c} = 0.6$. The facesheets significantly increase the weight of the structure but provide limited capability for energy dissipation.

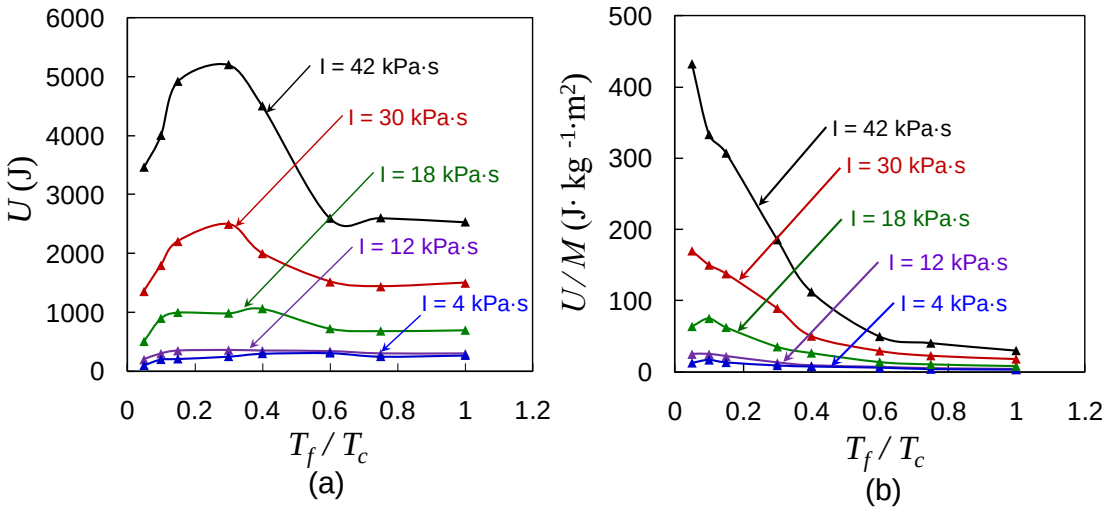

Figure 4 (a) Energy dissipated in the entire structure as a function of T_f/T_c, (b) energy dissipated per unit areal mass as a function of T_f/T_c.

Desirable Structural Configurations

The desired attributes for a sandwich structure is high energy dissipation capacity and high stiffness (small deflections). For energy dissipation, we consider the energy dissipated per areal mass. For stiffness, we consider maximum deflection of the structure. Figures 3 and 4 show that there is practically no performance benefit for structures with $T_f/T_c > 0.6$. Figures 4 (a) and (b) show that the highest energy dissipation capacity occurs for $0.15 < T_f/T_c < 0.4$. Figure 3 shows increases in facesheet thickness are most effective for $0.05 < T_f/T_c < 0.3$. Accounting for both factors, the most desirable range for facesheet thickness is T_f/T_c between 0.15 and 0.4 for a given core configuration.

Conclusions

The responses to underwater impulsive loads of composite sandwich plates consisting of glass-fiber reinforced epoxy facesheets and PVC foam core with different facesheet-thickness-to-core-thickness ratios are analyzed. The configuration studied is that used in experiments being carried out in the Underwater Shocking Loading Simulator recently developed at Georgia Tech. For comparison purposes, all material properties and core dimensions are kept constant. A fully dynamic 3D finite element model is developed for the experimental configuration, accounting for impulsive loading generation and the dynamic response processes of the structure and water. Deformation and failure mechanisms considered are core crushing, facesheet damage, and core-facesheet separation and contact. Calculations show the distinct response regimes of the structures, as measured by energy dissipated and the maximum deflection. It is found that under the loading conditions and for the material systems analyzed, there is a range of facesheet thickness in which planar sandwich structures offer the best performance. Specifically, structures with facesheet-thickness-to-core-thickness ratios between $0.15-0.4$ provide the most efficient use of material in terms of both energy dissipation capacity and rigidity. The insight gained here provides guidelines for the design of structures for which response to water-based impulsive loading is an important consideration. It is important to note that the analysis reported here concerns only one structural configuration, one combination of core and facesheet materials, and one core size. More extensive analyses and experimental verification are needed to determine the applicability of the findings to sandwich structures of different geometries, sizes and materials.

Acknowledgement

The authors gratefully acknowledge support by the Office of Naval Research through grant numbers N00014-09-1-0808 and N00014-09-1-0618 (program manager: Dr. Yapa D. S. Rajapakse). Calculations are carried out on the HPC cluster in the DPRL at Georgia Tech.

References

1. Steeves, C.A. and N.A. Fleck, *Collapse mechanisms of sandwich beams with composite faces and a foam core, loaded in three-point bending. Part II: experimental investigation and numerical modelling.* International Journal of Mechanical Sciences, 2004. **46**(4): p. 585-608.
2. Tagarielli, V.L., V.S. Deshpande, and N.A. Fleck, *The dynamic response of composite sandwich beams to transverse impact.* International Journal of Solids and Structures, 2007. **44**(7-8): p. 2442-2457.
3. Schubel, P.M., J.J. Luo, and I.M. Daniel, *Impact and post impact behavior of composite sandwich panels.* Composites Part a-Applied Science and Manufacturing, 2007. **38**(3): p. 1051-1057.
4. Nemes, J.A. and K.E. Simmonds, *Low-Velocity Impact Response of Foam-Core Sandwich Composites.* Journal of Composite Materials, 1992. **26**(4): p. 500-519.
5. Mines, R.A.W., C.M. Worrall, and A.G. Gibson, *The Static and Impact Behavior of Polymer Composite Sandwich Beams.* Composites, 1994. **25**(2): p. 95-110.
6. J. L. Abot, I.M.D., *Composite sandwich beams under low velocity impact.* Proc. of AIAA Conf. , Seattle, 2001.
7. Schubel, P.M., J.J. Luo, and I.M. Daniel, *Low velocity impact behavior of composite sandwich panels.* Composites Part a-Applied Science and Manufacturing, 2005. **36**(10): p. 1389-1396.
8. Wei, Z., et al., *Analysis and interpretation of a test for characterizing the response of sandwich panels to water blast.* International Journal of Impact Engineering, 2007. **34**(10): p. 1602-1618.
9. LeBlanc, J. and A. Shukla, *Dynamic response and damage evolution in composite materials subjected to underwater explosive loading: An experimental and computational study.* Composite Structures, 2010. **92**(10): p. 2421-2430.
10. Arora, H., Hooper, P. and Dear, J.P., *Blast and other high rate loading composite sandwich materials.* 9th International Conf on Sandwich Structures (ICSS-9), Ravichandran, G. ed, California Institute of Technology, Pasedena, USA (June 2010), Key-note paper MA3.1., 2010.
11. Espinosa, H.D., S. Lee, and N. Moldovan, *A novel fluid structure interaction experiment to investigate deformation of structural elements subjected to impulsive loading.* Experimental Mechanics, 2006. **46**(6): p. 805-824.
12. Horacio D. Espinosa , D.G., Félix Latourte and Ravi S. Bellur-Ramaswamy *Failure Modes in Solid and Sandwich Composite Panels Subjected to Underwater Impulsive Loads.* 9th International Conference on Sandwich Structures, ICSS9, 2010.
13. McShane, G.J., et al., *Dynamic rupture of polymer-metal bilayer plates.* International Journal of Solids and Structures, 2008. **45**(16): p. 4407-4426.
14. Dharmasena, K., et al., *Dynamic response of a multilayer prismatic structure to impulsive loads incident from water.* International Journal of Impact Engineering, 2009. **36**(4): p. 632-643.
15. DIAB Inc., S.D., DeSoto, Texas 75115, USA http://www.diabgroup.com/europe/literature/e_pdf_files/man_pdf/H_man.pdf Accessed 5 May 2011.
16. Tagarielli, V.L., V.S. Deshpande, and N.A. Fleck, *The high strain rate response of PVC foams and end-grain balsa wood.* Composites Part B-Engineering, 2008. **39**(1): p. 83-91.
17. Zhang, J., et al., *Constitutive modeling of polymeric foam material subjected to dynamic crash loading.* International Journal of Impact Engineering, 1998. **21**(5): p. 369-386.
18. Hibbit, Karlsson, and Sorensen, *Abaqus/Explicit User's Manual, Version 6.9.* 2009.
19. Deshpande, V.S. and N.A. Fleck, *Isotropic constitutive models for metallic foams.* Journal of the Mechanics and Physics of Solids, 2000. **48**(6-7): p. 1253-1283.
20. Hashin, Z., *Failure Criteria for Unidirectional Fiber Composites.* Journal of Applied Mechanics-Transactions of the Asme, 1980. **47**(2): p. 329-334.
21. Camanho, P.P., C.G. Davila, and M.F. de Moura, *Numerical simulation of mixed-mode progressive delamination in composite materials.* Journal of Composite Materials, 2003. **37**(16): p. 1415-1438.